

OSCILLATION AND FIRE AREA SHRINKAGE PHENOMENA OF WOOD CRIB AND HEPTANE POOL IN VENTILATION-CONTROLLED COMPARTMENT FIRES

Y. Utiskul^a and J. G. Quintiere^b

^aArupFire, Arup North America Ltd, Los Angeles, CA 90066 USA

^bDepartment of Fire Protection Engineering, University of Maryland, College Park, MD 20742 USA

ABSTRACT

To predict the effect of fire on the structures, one needs to understand physics of the fire growth in a compartment as to how the fuel interacts with the flame and its surroundings. This study explores these effects and applies them to the common fuel configurations such as pool and crib fires. An experimental program for single-wall-vent compartment using wood crib and heptane pool as fuels is carried out to explore a full range of phenomena associated with under ventilated compartment fires: extinction, oscillation, fire area shrinkage, and response of fuel to thermal and oxygen effects. A single-zone compartment fire model is developed along with a fuel mass loss rate model that accounts for the thermal enhancement, oxygen-limiting feedback, and the fuel type and configuration. The simulation from the model is able to capture these phenomena and shows good agreement with the experiments. Some generalities of the fuel mass loss rate and compartment gas temperature are presented using the experimental results and the model simulations. From the simulation, the fire area shrinkage can be the reason for the fuel mass loss rate to follow the same trend as the burning rate in ventilation-controlled fires. The developed model has a potential to give burning time and temperature in a fire for any fuel, scale and ventilation.

INTRODUCTION

A *fully-developed fire* is the stage of fire where all available fuels become involved and the fire burns at its maximum potential according to the limit amount of the available fuel (*fuel-controlled fire*) or the available air supply (*ventilation-controlled fire*). In most buildings, fires in common residential and office spaces become ventilation-controlled when a fully-developed stage is reached. In ventilation-controlled fires, all available fuel gases are not consumed by the flames and these gases can burn as they pass through the openings causing the flames to emerge windows and doors. To predict the maximum temperature and fire duration required for structural fire protection design, the *burning rate* and the *fuel mass loss rate* must be correctly calculated by taking into account for the fuel response to the thermal feedback enhancement from the enclosure and the vitiated oxygen effects. Unsteady fire behavior such as flame oscillation¹ and fire area shrinkage (burning area in ventilation-limited fires²) must also be taken into consideration as these phenomena affect the heat transfer to the fuel package and hence change the mass loss rate. Current design tools including correlations and mathematical fire models do not address the fuel response; therefore the burning time and temperature may not be properly predicted. This paper presents a study that may fulfill the incompleteness of the current design tools by establishing a single-zone fire model that addresses the fuel response and the unsteady behavior in ventilation-controlled fires and comparing the model to the observations from small-scale experiments.

COMPARTMENT BURNING RATE AND FUEL BEHAVIOR

The burning rate is defined as the rate at which the fuel, usually but not exclusively in the gas-phase, is consumed by the chemical reaction within the enclosure. The burning rate plays a significant

role in compartment fire because it represents how much energy is released into the system. The energy release rate or fire power, \dot{Q} , within the enclosure is given as

$$\dot{Q} = \Delta h_c \dot{m}_b, \quad [1]$$

where \dot{m}_b is the burning rate and Δh_c is the heat of combustion per unit mass of fuel. In some literature, however, the term burning rate was used to describe the fuel mass loss rate. While these two rates may arguably follow the same trend; they have completely different meaning. The fuel mass loss rate refers to the rate at which a condensed-phase fuel is decomposed to gases due to the energy transferred from its surrounding heat sources such as flames, hot gas, and enclosure walls. We can describe the relationship for the mass loss rate and the burning rate as follow:

$$\dot{m}_b = \begin{cases} \dot{m}_F & ; \phi < 1 \\ \dot{m}_o / s & ; \phi \geq 1 \end{cases} \quad [2]$$

where \dot{m}_o is the incoming air flow rate, \dot{m}_F is the fuel mass loss rate, s is the stoichiometric mass of air to fuel ratio and the global equivalence ratio $\phi = \dot{m}_F / \dot{m}_o \cdot s$. In compartment fire experiments the fuel mass loss rate can be directly measured using weighing cells to track the weight of the fuel over time; however, measurement for the burning rate may not be done directly especially in the under-ventilated condition. In order to predict the burning rate, the fuel mass loss rate must be accurately known as appears in Eq 2. This is always true even for the under-ventilated condition, where burning depends on available air, because the fuel mass loss rate also determines the burning state. The fuel mass loss rate can be given as³

$$\dot{m}_F = \dot{m}_{F,o}'' A_{F,b} \frac{Y_{ox,l}}{Y_{ox,o}} + \frac{\dot{q}_{External}}{L}, \quad [3]$$

where $\dot{m}_{F,o}''$ is the free burning rate or fuel mass loss rate in opened environment per unit area, $A_{F,b}$ is the burning fuel exposed area, $Y_{ox,l}$ is the oxygen mass fraction feeding the flame, $Y_{ox,o}$ is the oxygen fraction in the free burning generally equals to 0.233, L is the heat of gasification depending on the fuel type, and $\dot{q}_{External}$ is the total external heat feedback from smoke and compartment wall surfaces. The first term on the right hand side of Eq (3) represents the *vitiated oxygen effect* on the flame heat flux^{4,5} and the second term is responsible for the *thermal feedback* from smoke and compartment wall surfaces.

A common correlation for the free burning rate per unit area of large liquid pool fires ($D > 0.2$ m) is given as⁶ $\dot{m}_{F,o}'' = \dot{m}_{F,max}'' (1 - e^{-\kappa_f L_f})$, where $\dot{m}_{F,max}''$ is the asymptotic value for fuel mass loss rate, κ_f is the flame absorption coefficient depending on the fuel type, and L_f is the mean beam length. For a cylindrical shape flame⁷ with a diameter (D), $L_f = 0.66D$.

A correlation describing the time-average free burning rate per unit exposed area for wood cribs, A_F , was established by Heskestad⁸ as $\dot{m}_{F,o}'' = 0.968 C_w b^{-1/2} (1 - \exp(-(sb)^{1/2} A_{C,o} / 0.02 A_F))$, where b is the thickness dimension of a stick, s is the spacing between sticks, $A_{C,o}$ is the cross-sectional area of the vertical crib shafts, and C_w is the empirical wood crib coefficient given by Block⁹. The total external radiation feedback can be given as $\dot{q}_{External} = \dot{q}_{Ext,b} + \dot{q}_{Ext}$, where $\dot{q}_{Ext,b}$ and \dot{q}_{Ext} are the net radiation feedback to the flaming fuel area and non-flaming fuel area respectively and can be given as follows

$$\begin{aligned} \dot{q}_{Ext,b} &= F_g (1 - \varepsilon_f) \varepsilon_g A_{F,b} (T^4 - T_o^4) + F_w (1 - \varepsilon_f) (1 - \varepsilon_g) A_{F,b} (T_w^4 - T_o^4) \\ \dot{q}_{Ext} &= F_g \varepsilon_g (A_F - A_{F,b}) (T^4 - T_v^4) + F_w (1 - \varepsilon_g) (A_F - A_{F,b}) (T_w^4 - T_v^4) \end{aligned}, \quad [4]$$

where T is the compartment gas temperature, T_o is the ambient temperature, T_w is the wall temperature, T_v is the fuel vaporization temperature or the fuel surface temperature, F_g is the shape factor from the fuel to the compartment gas, F_w is the shape factor from the fuel to the walls, and A_F is the total fuel surface area, ε_f and ε_g are the emissivity of the flame and the smoke respectively.

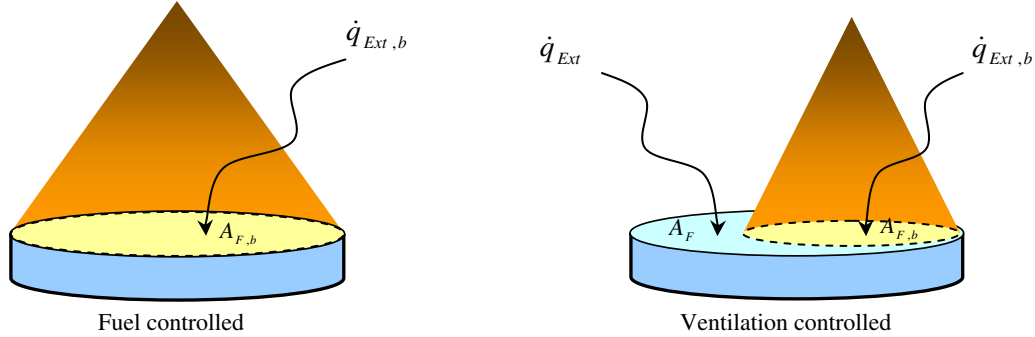


Figure 1: External radiation feedback on flaming and non-flaming surface area for a pool fire

BURNING AREA IN VENTILATION-CONTROLLED FIRES

Thomas and Bennetts¹⁰ observed flames partially burning over a series of liquid fuel trays in their experimental study on long and wide enclosures. They reported that after ignition the flame formed itself at the front of the fuel tray closest to the vent. Later, when the fuel in the front tray was exhausted, the flame moved towards the rear of the enclosure (away from vent) to the next adjacent tray. This behavior takes place because the compartment reaches the ventilation-controlled condition where the burning is controlled by the amount of supplied air. We also experienced the same phenomena in our experiment programs with distributed fuel packages all over the floor. Motivated by such observations, we offer a reason why only a certain amount of fuel area will react with the limited amount of air supply. The flame therefore burns only on this certain area to match its needed fuel, and then “moves” when the local fuel is exhausted. The following analysis is put forth to estimate the burning area in ventilation-controlled fire². From Eq 3 and 5, the expression for the fuel burning rate can be given as

$$\dot{m}_b = \dot{m}_{F,o}'' A_{F,b} \frac{Y_{ox,l}}{Y_{ox,o}} + \frac{\dot{q}_{Ext,b}'' A_{F,b}}{L} \quad [5]$$

Recall Eq 2 for the under ventilated condition and substitute into Eq 5 we have,

$$\frac{\dot{m}_o}{s} = \dot{m}_{F,o}'' A_{F,b} \frac{Y_{ox,l}}{Y_{ox,o}} + \frac{\dot{q}_{Ext,b}'' A_{F,b}}{L}. \quad [6]$$

If we assume that the fuel burns in a circular shape i.e. $A_{F,b} = \pi D_b^2/4$, upon rearranging we have

$$\frac{\pi D_b^2}{4} = \frac{\dot{m}_o}{s} \left/ \left(\dot{m}_{F,o}'' \frac{Y_{ox,l}}{Y_{ox,o}} + \frac{\dot{q}_{Ext,b}''}{L} \right) \right. \quad [7]$$

Substituting the emissivities of the smoke and the flame with $D = D_b$ into the $\dot{q}_{Ext,b}''$ term, we can iteratively solve for the burning diameter, D_b , and hence obtain the fuel burning area.

NEAR VENT MIXING

To predict the fuel mass loss rate, the concentration of the oxygen feeding the flame, $Y_{ox,l}$, needs to be estimated. In room fires when the vent is small and the smoke layer descends close to the floor, the entering cold fresh air stream can be contaminated by the smoke due to the buoyancy and shear mixing¹¹ occurring near the vent. This phenomenon, called vent mixing, leads to the reduction in oxygen feeding the flame and it is therefore an important factor to explain the effect of ventilation on the fuel mass loss rate in the compartment fires. A method of characterizing the near vent mixing behavior has not been well established; however, some investigations have been carried out. Zukoski et al.^{12, 13} developed a correlation for the mixing rate from saltwater simulation experiments. Zukoski's correlation was based on an assumption that the cold incoming flow through the opening would behave like a point source buoyant plume entraining the hot gas in the upper layer and then descending downward to the lower layer. In this study, the mixing model was investigated based on Quintiere and McCaffrey¹⁴ that the incoming cold air behaved like a jet entering the doorway with a characteristic velocity and diffusing downward because of buoyancy. While the cold air descended, the surrounding hot gas was entrained with a velocity that is proportional to the incoming flow characteristic velocity. From this concept, we obtain a ratio of mass entrained to the total incoming mass flow rate or mixing ratio as

$$\frac{\dot{m}_e}{\dot{m}_o} \sim \left(\frac{T_o}{T}\right) \left(1 + \frac{N-S}{W_o}\right) \left(\frac{N-Z}{N-S}\right), \quad [8]$$

where \dot{m}_e is the mixing rate, W_o is the opening width, S is the sill height, Z is the smoke layer height, and N is the neutral plane height. Hence, we wish to obtain a correlation for the mixing ratio empirically in the form of Eq 8. Single-vent compartment fire experiments were conducted³ to establish the correlation for the mixing at the quasi-steady state. The fuel supply rate was controlled and the measurements include the oxygen concentration vertical profiles, gas temperature, smoke layer heights, and neutral plane height. From the steady-state conservation of oxygen, the mixing ratio, \dot{m}_e/\dot{m}_o , can be estimated from the measured oxygen concentration in the lower and upper layer as $\dot{m}_e/\dot{m}_o = (Y_{ox,o} - Y_{ox,l}) / (Y_{ox,l} - Y_{ox,u})$. From the experiments, we found that the mixing ratio is well correlated with Eq 6 and a linear relationship up to an apparent asymptote for the mixing ratio of 1.28. This can be put into an expression for the mixing ratio as follows:

$$\begin{aligned} \dot{m}_e/\dot{m}_o &= 1.14 \cdot \Psi & \text{for } \Psi < 1.1 \\ \dot{m}_e/\dot{m}_o &= 1.28 & \text{for } \Psi \geq 1.1 \end{aligned} \quad [9]$$

where Ψ represents the right hand side of the Eq 8. A well-mixed condition in the compartment fire is defined when the layer interface or the smoke is close to the floor. The opening geometry and fire size plays an important role on the location of the layer interface³. When this condition prevails, the properties of the gas in the compartment are said to be uniform and a single zone model can be effectively used to predict the gas temperature and species in the compartment. Nevertheless, in reality a sharp gradient of the oxygen concentration still exists near the floor. In other words, the oxygen that is feeding the flame is not the same as in the bulk smoke layer even though the smoke layer is close to the floor. In order to overcome this, the mixing can be used as a mechanism to help defining the local oxygen feeding the flame in a single zone model. We choose to use a constant maximum value of 1.28 for the mixing ratio as suggested for the well-mixed compartment fires with a single-wall-vent configuration. This limit would apply when the layer is close to the floor.

SINGLE-ZONE MODEL

To create a complex model that could provide an absolute prediction on every aspect of the compartment fire behavior may not be possible at this time. Nevertheless, a simple, yet beneficial model could be derived in order to demonstrate the important mechanisms. For a large fire at the fully-developed

stage, the compartment is often filled with the smoke and the layer interface is close to the floor. Such a condition can be termed the *well-mixed* stage where the gas is assumed to have uniform properties throughout the compartment. A single-zone model assumption is usually suitable for this type of fires. Assuming uniform property, we have conservation relationships as

$$\text{Mass:} \quad \rho_o T_o V \frac{d}{dt} (1/T) + \dot{m} - \dot{m}_o - \dot{m}_F = 0 \quad [10]$$

$$\text{Oxygen:} \quad \rho_o T_o V \frac{d}{dt} (Y_{ox}/T) + \dot{m} Y_{ox} - \dot{m}_o Y_{ox,o} = -\dot{Q}/\Delta h_{ox} \quad [11]$$

$$\text{Energy:} \quad \frac{V}{\gamma-1} \frac{dP}{dt} + c_p \dot{m} T - c_p \dot{m}_o T_o - c_p \dot{m}_F T_F = \dot{Q} - \dot{q}_{wall} - \dot{q}_{vent} \quad [12]$$

Here \dot{m} is the outflow rate, \dot{m}_o is the inflow rate, \dot{m}_F is the fuel mass loss rate, Δh_{ox} is the heat of combustion per unit mass of oxygen, V is the enclosure volume, \dot{q}_{wall} is the heat transfer to the boundaries, and \dot{q}_{vent} is the heat loss through the opening via radiation, and $\gamma = c_p / c_v$. Subscript “o” represents ambient condition. By letting the neutral plane be the reference level, mass flow through the vent between the height ($z_a < z < z_b$) is given as

$$\text{Vent Flow:} \quad \dot{m}_i = \frac{2}{3} C_d W_o \sqrt{2g\rho_i(\rho_o - \rho)} (z_b^{3/2} - z_a^{3/2}), \quad [13]$$

where z_a and z_b are measured from the reference height. The convection heat transfer from gas to the wall is simply

$$\dot{q}_{conv} = h_c A_w (T - T_{w,0}), \quad [14]$$

where $T_{w,0}$ is the wall surface temperature, A_w is the wall total surface area, and h_c is the convective heat transfer coefficient taken from an empirical correlation developed in a recent scale modeling study for compartment heat transfer by Veloo¹⁵. This correlation is consistent with Tanaka and Yamada¹⁶ and is developed for a higher range of temperature. It is given as

$$\frac{h_c}{\rho_o c_p (gl)^{1/2}} = \begin{cases} 3.5 \times 10^{-3} & ; \theta < 2.2 \\ 16 \times 10^{-3} \theta - 31.7 \times 10^{-3} & ; \theta \geq 2.2 \end{cases} \quad [15]$$

where l is the compartment height and $\theta = (T - T_o) / T_o$. Assuming a grey uniform-temperature wall, the radiation exchange between gas and the compartment wall⁷ is

$$\dot{q}_{rad} = \frac{A_w \sigma (T^4 - T_{w,0}^4)}{1/\epsilon_g + 1/\epsilon_w - 1}. \quad [16]$$

As for the heat conduction through the boundary, by spatially discretizing a transient one-dimensional heat equation with the centered difference scheme into n elements, we have a system of algebraic ordinary differential equations as follows:

$$\left(\begin{array}{l} \frac{dT_{w,1}}{dt} = \frac{k_{w,2}(T_{w,2} - T_{w,1}) - k_{w,1}(T_{w,1} - T_{w,0})}{\Delta x^2 \rho_w c_{pw,1}} \\ \frac{dT_{w,2}}{dt} = \frac{k_{w,3}(T_{w,3} - T_{w,2}) - k_{w,2}(T_{w,2} - T_{w,1})}{\Delta x^2 \rho_w c_{pw,2}} \\ \vdots \\ \frac{dT_{w,n}}{dt} = \frac{k_{w,n+1}(T_{w,n+1} - T_{w,n}) - k_{w,n}(T_{w,n} - T_{w,n-1})}{\Delta x^2 \rho_w c_{pw,n}} \end{array} \right) \text{ and } \begin{array}{l} \frac{-k_{w,1}(T_{w,1} - T_{w,0})}{2\Delta x} = h_c(T - T_{w,0}) + \varepsilon_g \sigma (T^4 - T_{w,0}^4) \\ \frac{-k_{w,n}(T_{w,n+1} - T_{w,n-1})}{2\Delta x} = h_{c,ambient}(T_{w,n} - T_o) \end{array} \quad [17]$$

A flame extinction condition can be defined by a flammability line that is based on a critical flame temperature below which the extinction occurs and no energy is generated into the system. The flame temperature T_f is given as¹⁷

$$c_p(T_f - T_l) = \frac{\Delta h_c - L + c_p(T_v - T_l) + \frac{\dot{q}_{Ext,b}''}{\dot{m}_b}}{1 + (r/Y_{ox,l})}, \quad [18]$$

where r is the stoichiometric oxygen to fuel ratio given by, $Y_{ox,l}$ and T_l and are the local oxygen level and temperature of the gas that is feeding the flame respectively. Based upon the extinction flame temperature, the criteria for energy release rate (or burning rate) given in Eq 1 is expressed as

$$\dot{m}_b = \begin{cases} \dot{m}_F & ; Y_{ox} > 0 \text{ and } T_f > 1300^\circ\text{C} \\ \frac{\dot{m}_o Y_{ox,o}}{r} & ; Y_{ox} = 0 \text{ and } T_f > 1300^\circ\text{C} \\ 0 & ; T_f \leq 1300^\circ\text{C} \end{cases}, \quad [19]$$

where \dot{m}_F is given in Eq 3. Lastly from the mixing ratio, $\dot{m}_e/\dot{m}_o = 1.28$, described previously, $Y_{ox,l}$ and T_l can be calculated as $Y_{ox,l} = \frac{Y_{ox,o} + (\dot{m}_e/\dot{m}_o)Y_{ox,u}}{1 + (\dot{m}_e/\dot{m}_o)}$ and $T_l = \frac{T_o + (\dot{m}_e/\dot{m}_o)T_u}{1 + (\dot{m}_e/\dot{m}_o)}$ respectively.

COMPARTMENT FIRE EXPERIMENT AND MODEL APPLICATION

A series of experiments using a small-scale compartment was conducted in which the quantity and configuration of the fuel were varied under natural ventilation condition of various doorway and window widths. The compartment was built with 2.54 cm (1 inch) thick Type-M Kaowool board. The compartment inner size was measured 40 cm × 40 cm × 120 cm (height × width × depth). Two kinds of the single-wall-vent, doorway-like and window-like, were used. The vent height and the sill height were designed such that they represented the common doorway and widow height in real buildings. The measurements are comprised of fuel mass loss rate, gas temperatures, oxygen concentrations, heat flux to wall surface, and differential pressure near vent. Figure 2 shows the section view of the compartment and the measurement layout. The fuel configurations selected here were the *crib* fire and the *pool* fire. Two types of wood, Oak and Pine, were selected as the material for the crib fire. The crib configurations were designed to have surface controlled burning. Heptane (C₇H₁₆) was used for the pool fire tests. Descriptions for wood crib and pool size are presented in Table 1. A range of opening sizes and the fuel loads were selected to span over the ventilation factor, $A_o \sqrt{H_o} \rho_o \sqrt{g} / A_F$, to represent the full range of real fire conditions. Table 2 provides the experimental conditions. From the experiment, the burning can be categorized into 3 cases based on the observed behavior and the global equivalence ratio. The 3 cases are:

Case 1: Steady well-ventilated burning. This is the case where vent is large and the global equivalence ratio is less than one. The flame stabilized above the fuel, and the oxygen in the upper layer is above zero.

Case 2: Steady under-ventilated burning. In this case the opening size is reduced and the global equivalence ratio is less than one. The burning is ventilation-limited and the fire area shrinkage occurs. Oxygen in the upper layer is at or near zero. The oscillating flame may take place if the extinction criterion, depending on the local temperature and oxygen, is reached. But the oscillation is only a transient stage for this case and the flame eventually reaches the steady stage where no oscillation occurs and become under-ventilated.

Case 3: Unsteady under-ventilated burning. In this case the opening size is the smallest among all cases. Periodic oscillating flame is observed. The global equivalence ratio is less than one; however, the oxygen in the upper layer is above zero. In this case the extinction criterion is reached and the oscillating flame occurs until the fuel is exhausted. Throughout the burning, the flame does not consume all the oxygen available. Figure 6 shows video capture and results from Crib2D28x5.

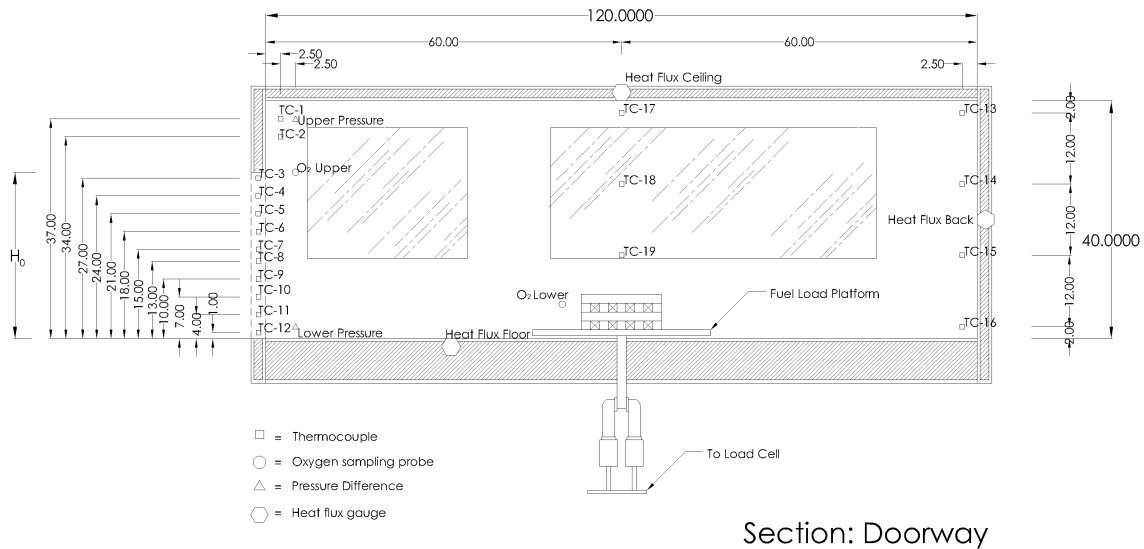


Figure 2: Schematic of the compartment and measurement layout

Table 1: Wood crib and heptane pool description

Crib	b (m)	n_i	n_j	L_i (m)	L_j (m)	N	Type	Pool	Diameter (m)	Heptane volume (ml)
1	0.012	4	7	0.3	0.15	5	Pine	1	7x0.138, 3x0.147	90 (each pan)
2	0.01905	4	4	0.15	0.15	5	Pine	2	0.245	300
3	0.012	5	5	0.15	0.15	4	Pine			
4	0.011	9	9	0.25	0.25	5	Oak			
5	0.022	5	9	0.414	0.207	3	Oak			

Table 2: Experimental conditions

Test	H_o (m)	W_o (m)	S (m)	A_F	Test	H_o (m)	W_o (m)	S (m)	A_F
Crib1D28x15	0.28	0.15	0.00	0.234	Crib3D28x30	0.28	0.30	0.00	0.119
Crib1W14x20	0.14	0.20	0.14	0.234	Crib3D28x40	0.28	0.40	0.00	0.119
Crib1W14x32	0.14	0.32	0.14	0.234	Crib3W14x32	0.14	0.32	0.14	0.119
Crib2D28x05	0.28	0.05	0.00	0.185	Crib4D28x15	0.28	0.15	0.00	0.403
Crib2D28x15	0.28	0.15	0.00	0.185	Crib5D28x15	0.28	0.15	0.00	0.414
Crib2D28x30	0.28	0.30	0.00	0.185	Pool1D28x15	0.28	0.15	0.00	0.1557
Crib2D28x40	0.28	0.40	0.00	0.185	Pool2D28x15	0.28	0.15	0.00	0.0472
Crib2W14x06	0.14	0.06	0.14	0.185	Pool2D28x30	0.28	0.30	0.00	0.0472
Crib2W14x32	0.14	0.32	0.14	0.185					

We will discuss further on each burning category along with the dynamic results and the model predictions from the selected test that represents such category. Here the measurement is shown in gray and the prediction is in dark solid line. Figure 3 shows the measurements and predictions from Case 1 (Crib2D28x30). The predicted flame effect (the first term on the right-hand-side of Eq 3) and the thermal

feedback (the second term on the right-hand-side of Eq 3) are also presented. Gas temperature data were taken at the opening (TC 3 to TC12). In this case the model seems to slightly underestimate the mass loss rate the gas temperature; although, it remains good agreement. This could be because the smoke layer height in this case is located well above the floor where the assumption for the single zone may not be well satisfied.

Figure 4 shows the results of wood crib (Crib1W14x32) for Case 2. In this test as the fire became ventilation-controlled (oxygen in the upper layer reached zero), the fire area shrinkage occurred. This behavior was observed in both experiment and prediction. An attempt to estimate the shrinking burning area has been made from video observation and also presented along with the prediction from the model. The model matches well with the mass loss rate and the maximum gas temperature measured at the vent. In this case the compartment fuel mass loss rate is lower than its free burning value because of two reasons: 1) the oxygen effect is more dominant than the thermal effect and 2) the reduction in burning area due to ventilation limited condition.

Similar fire area shrinkage behavior is presented in Figure 5 for heptane pool fire (Pool1W28x15). In this test a series of 10 heptane pans were distributed over the load platform. The ignition was started at the fuel pan located closest to the vent and the flame propagated through all other pans almost immediately. Since the heptane fuel exposing area was large and the gasified fuel was more than a stoichiometric need, the burning condition reached the ventilation-limited condition quickly. This is shown by the measured oxygen approaching near zero percent at about 20 s after ignition. Shrinking in burning area was observed and the flame was then stabilized near the vent. This case is an example of the classical ventilation-limited burning where the most of the flame burns outside of the vent. Note that the gas temperature measured across the vent in this case is basically the flame temperature. Despite the enhancement from enclosure thermal feedback, the measured fuel mass loss rate is much lower than the free burning rate because of the reduction in the burning area and the change of the flame location. As for the model prediction in this case, the model shows a sharp peak in the fuel mass loss rate about 5 s, then a sharp decrease due to the ensuing ventilation-limited condition. The shrinking in burning area predicted by the model is consistent to the estimation made from the video observations and the reduction in mass loss rate due to area shrinking is well captured. Since the fire area shrinkage is evident in the ventilation-limited fire as shown by our result, this phenomenon can be responsible for the reduction of the fuel mass loss rate in the ventilation-limited condition and can explain why the fuel mass loss rate follows the same trend as the “burning rate” in ventilation-limited fires.

The unsteady flames categorized in Case 3 usually occur in a very low ventilation condition and can appear in several forms such as a periodically *oscillating flame* stabilizing above the fuel bed, and a *ghosting flame* that drifts away from the fuel bed with temporally extinction. Takeda and Akita¹ have observed the unstable oscillation flames of methanol and PMMA pool in their compartment fire experiments, and identified the ventilation regime that these behaviors were seen. Chamchine et al.¹⁸ have observed this type of unsteadiness flame in their experiments using a hydrocarbon gas fuel. In this study, the unsteady flame of wood crib fires (Crib2D28x5) is presented in Figure 6. The oscillations, or on-off flame phenomena, were evident from the measurements of the pressure difference and the gas temperatures at the vent. We offer an explanation for this flame behavior as follows: As the oxygen concentration feeding the flame decreases the flame becomes weak⁴ and is almost extinguished, the compartment temperature also reduces. The sudden change in temperature causes the change in the differential pressure and induces the fresh air into the compartment. This fresh air then revitalizes the flame which later causes the sudden increase in temperature and again consumes most oxygen; hence the process repeats. As for the prediction in this case, the model gives a reasonably good simulation for both effects. It is able to capture the oscillating phenomenon as shown in the predicted mass loss rate and the pressure differences. Nevertheless, it is worth mentioning that although the oscillating flame phenomena involves the extinction and re-ignition events, the current single zone model uses the critical flame extinction criteria, Eq 18, for both events; a true ignition model has not been included in the current work.

In this case, although the global equivalence ratio is more than one, the oxygen in the upper layer from both measurement and prediction shows more than zero percent. This means that all oxygen is not consumed due to the temporary flame extinction. In other words, the flame reaches its extinction criteria before the ventilation limited condition prevails.

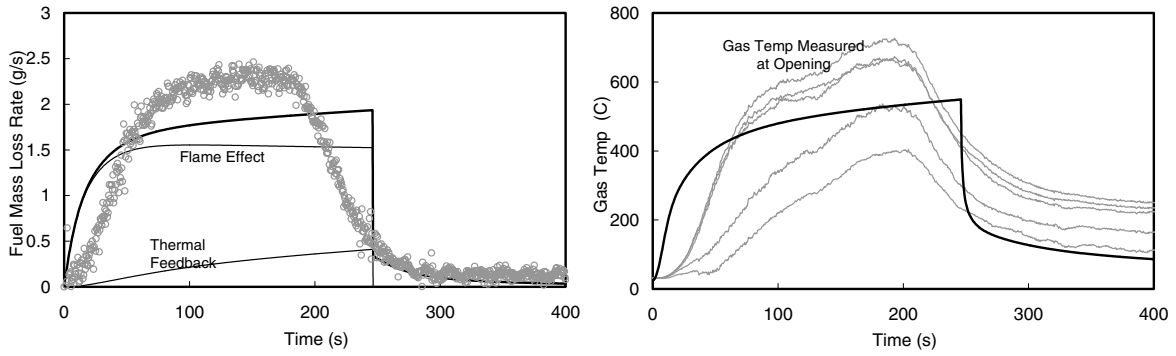


Figure 3: Experiment and prediction from Crib2D28x30-Case 1, GER = 0.45

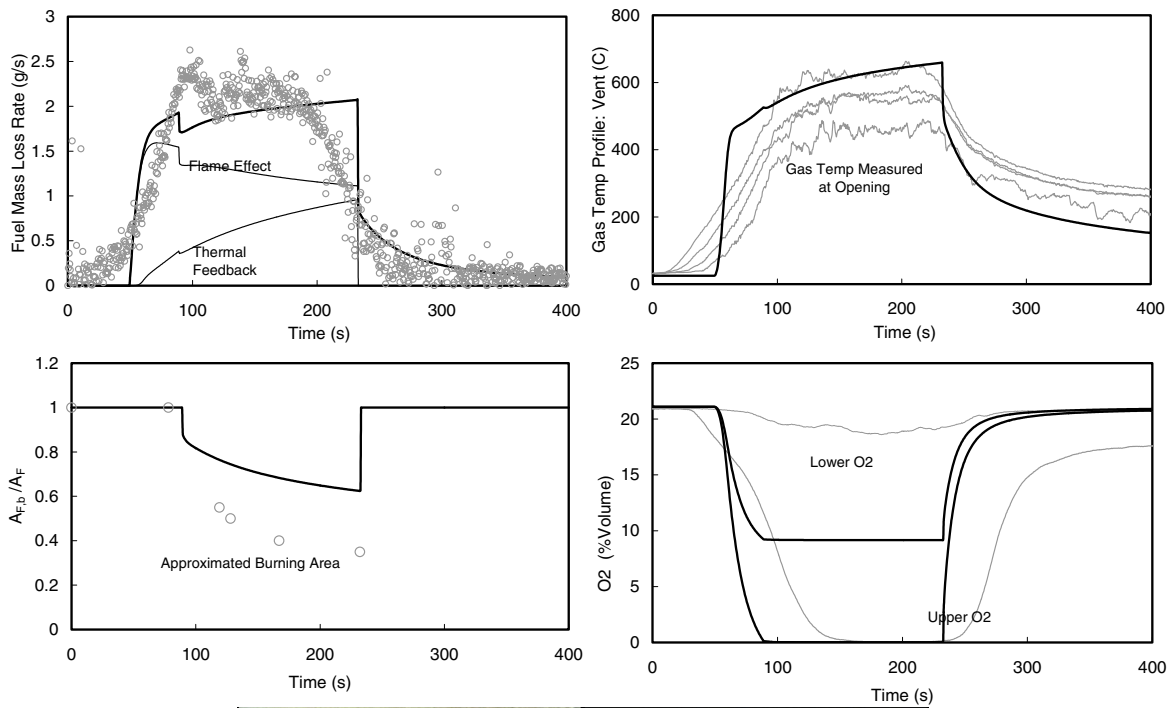


Figure 4: Experiment and prediction from Crib1W14x32-Case 2, GER = 1.2

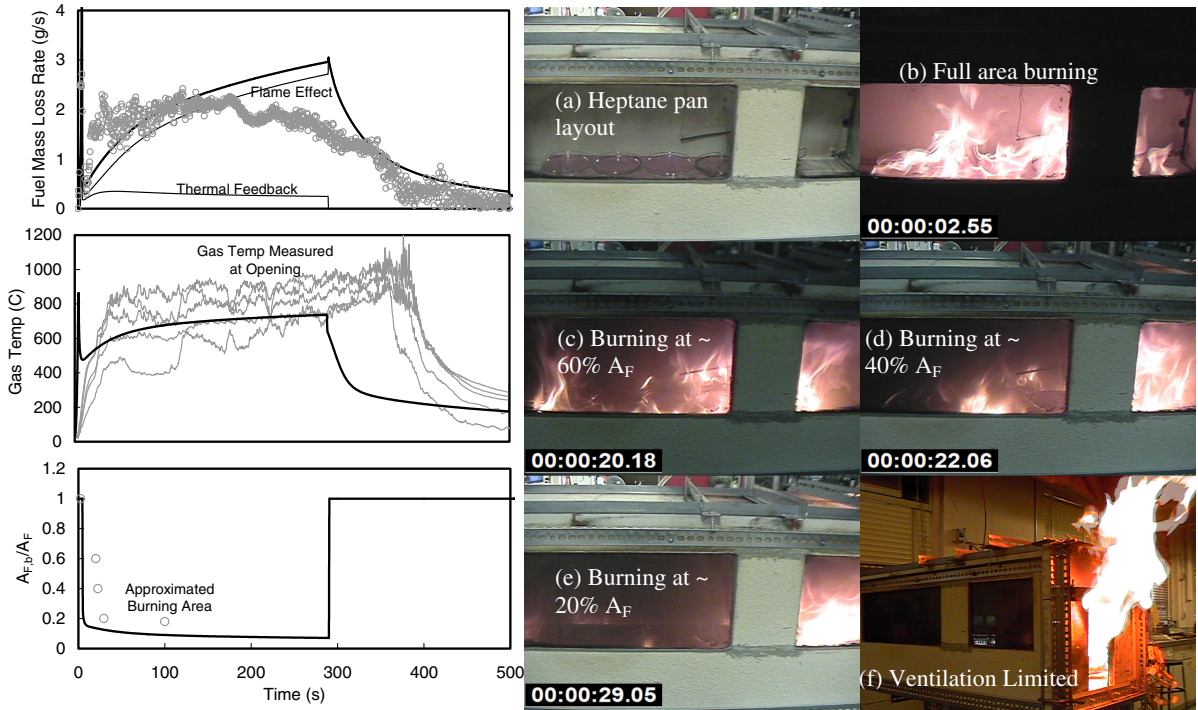


Figure 5: Experiment and prediction from Pool1W28x15-Case 2, GER = 3

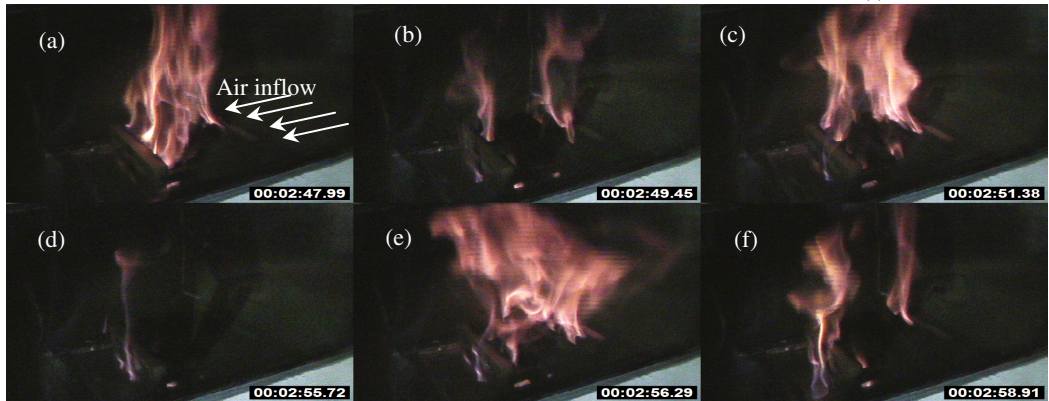
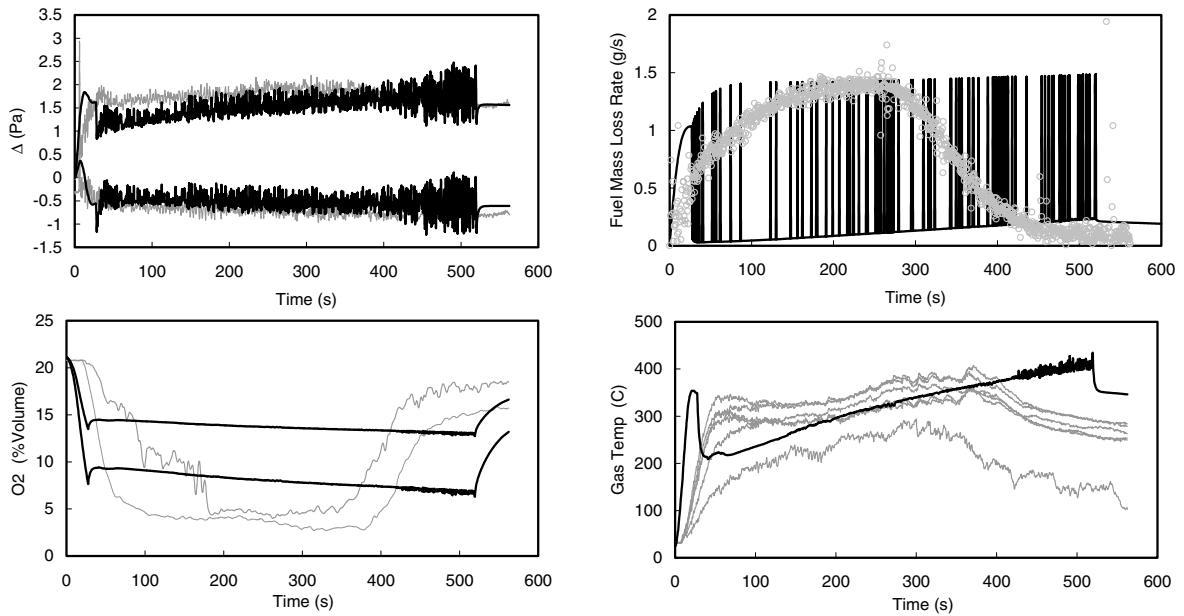


Figure 6: Experiment and prediction from Crib2D28x5-Case 3, GER = 1.5

In addition to the transient results, an average peak value was determined for the fuel mass loss rate and the upper layer gas temperature to present the experiment and the model prediction in a global perspective. The average peak value for both measured and predicted variables was determined in the following manner. The time interval corresponding to the fuel mass changing from 80 to 30 percent of its initial mass was identified. All variables were then numerically averaged over this time interval to yield the average peak values. Figure 7 presents the average peak value of the fuel mass loss rate in terms of the effect of the ventilation ($A_o\sqrt{H_o\rho_o\sqrt{g}/A_F}$) and the wall heat loss (A_s/A_F).

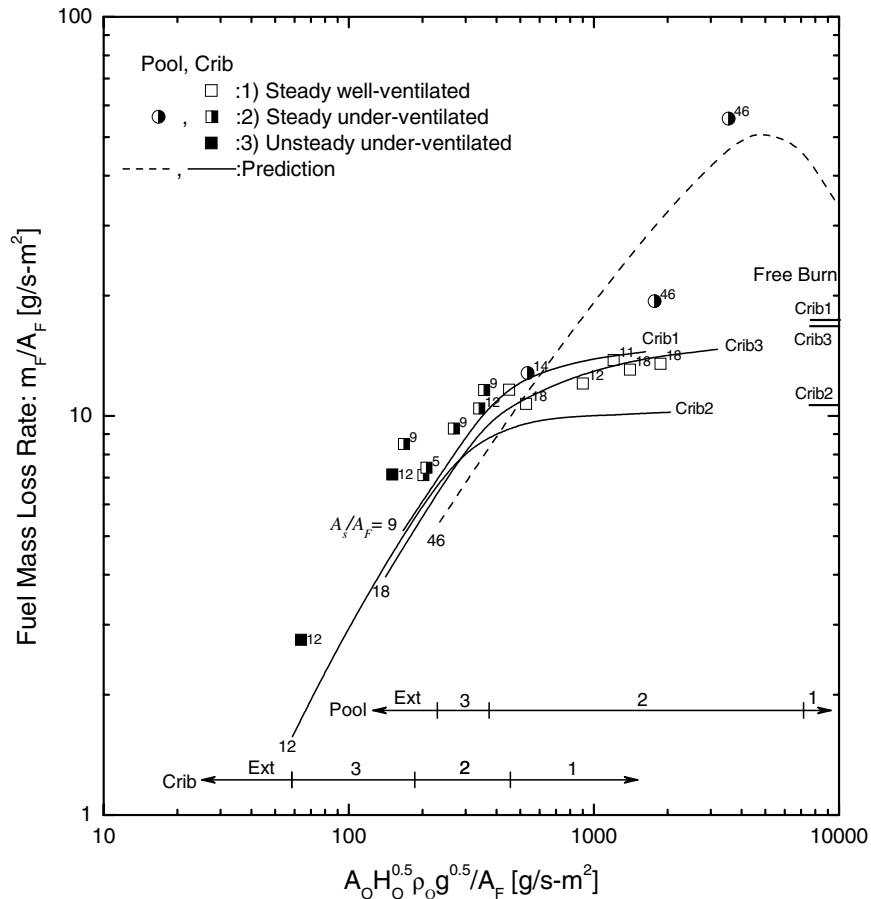


Figure 7: Dependence of the peak average fuel mass loss rate on ventilation and wall heat loss

The free burning rate is also presented on the right-vertical axis for each crib in Figure 7. The trend predicted by the model generally agrees well with the experiment for both wood crib and heptane fires. The regimes of burning (Case 1 to Case 3) based on the observation in the simulation are illustrated on the plot using the horizontal arrow-head line. The number marked on each regime corresponds to the case 1 to case 3 and the abbreviation “Ext” designates the complete flame extinction. As shown by the experiments and simulations on the figure, the burning behavior regime of the heptane pool and wood crib fire do not coincide with each other. For instance, at the same ventilation factor ($A_o\sqrt{H_o\rho_o\sqrt{g}/A_F}$) of $1000 \text{ g/m}^2\text{s}$, the pool fire is already in its ventilation-limited range while the crib fire is still in the well-ventilation regime. The prediction of the crib shows that in the well-ventilated regime (Case 1), the thermal feedback enhancement does not exhibit a strong effect on the mass loss rate and the flame (or oxygen) effect is more dominant as seen by the less value of the crib mass loss rate than its free burning rate. This is also consistent with the experimental result. In addition, no trend is observed for the area ratio, A_s/A_F , in the well-ventilated regime because the thermal effect is small and the crib mainly burns according to its free burning. In other words, for non-porosity-controlled cribs, the stick size is responsible for the mass loss rate of the different crib configuration in the well-ventilated regime. In the under-ventilated regime (Case 2 and 3), a general observation from the model and the experiment is that the mass loss rate decreases as

the ventilation decreases. However, the wood crib burning dependence on A_s / A_F becomes clearer from the simulation as the burning is now controlled by the air inflow, oxygen reduction in the lower layer and higher gas temperatures as the amount of fuel (A_F) is increased. Hence, without the scale differences, for ventilation-limited fires, the smaller the ratio A_s / A_F , the higher the mass loss rate.

CONCLUDING REMARKS

A single-zone fully-developed compartment fire model that accounts for the fuel type and configuration has been established. The model is capable of predicting the gas temperature and the fuel mass loss rate that can relate to the burn time in a fire for any fuel, scale and ventilation. The model shows good agreement with the experiment and is able to reveal the full range of phenomena associated with fully developed fires as observed in the experiment: response of fuel to thermal and oxygen effects, oscillation, and fire shrinkage area. Generally, the higher temperature and mass loss rate are achieved with the lower ratio of A_s / A_F . The fire area shrinkage can be the reason for the *fuel mass loss rate* to follow the same trend as the *burning rate* in ventilation-limited fires.

Acknowledgments

This study was supported by the National Institute of Standards and Technology and the John L. Bryan Chair Fund.

REFERENCES

- ¹ Takeda, H. and Akita, K. (1981) In *Symp Int Combust 18th*, Vol. 18 Combustion Institute, Waterloo, Ont, USA, pp. 519-527.
- ² Utiskul, Y. and Quintiere, J. G. (2005) In *Eighth IAFSS Symposium* Beijing, China.
- ³ Utiskul, Y. (2006) In *Fire Protection Engineering and Mechanical Engineering* University of Maryland, College Park, MD.
- ⁴ Tewarson, A., Lee, J. L. and Pion, R. F. (1981) In *Symp Int Combust 18th* Combustion Institute, Waterloo, Ont, USA, pp. 563 - 570.
- ⁵ Santo, G. and Delichatsios, M. A. (1982) Factory Mutual Research, Norwood, Massachusetts.
- ⁶ Babrauskas, V. (1983) *Fire Technology*, 251.
- ⁷ Karlsson, B. and Quintiere, J. G. (1999) *Enclosure Fire Dynamics*, CRS Press, Florida.
- ⁸ Heskestad, G. (1972) In *Symp Int Combust 14th* The Combustion Institute, PA, USA, pp. 1021-1030.
- ⁹ Block, J. A. (1970) In *13th Symposium (International) on Combustion* Combustion Institute, Salt Lake City, Utah, pp. 971-978.
- ¹⁰ Thomas, I. R. and Bennetts, I. D. (1999) In *Fire Safety Science-Proceedings of the Sixth International Symposium* France, pp. 941-952.
- ¹¹ Quintiere, J. G. (1995) In *SFPE Handbook of Fire Protection Engineering* National Fire Protection Association, pp. 3.125 - 3.133.
- ¹² Zukoski, E. E. (1978) California Institute of Technology, Pasadena, CA.
- ¹³ Lim, C. S., Zukoski, E. E., and Kubota, T. (1984) California Institute of Technology, Pasadena, CA.
- ¹⁴ Quintiere, J. G., McCaffrey, B.J. (1980) National Bureau of Standards, Washington, DC.
- ¹⁵ Veloo, P. (2006) In *Fire Protection Engineering* University of Maryland, College Park, pp. 127.
- ¹⁶ Tanaka, T. and Yamada, S. (1999) *International Journal on Engineering Performance-based Fire Codes*, **1**, 196-203.
- ¹⁷ Quintiere, J. G. and Rangwala, A. S. (2003) *Fire and Materials*, **28**, 387-402.
- ¹⁸ Chamchine, A. V., Makhviladze, G. M., Snegirev, A. and Graham, T. L. (2004) In *Interflam2004*, Vol. 1 Edinburgh, UK, pp. 73 - 82.